Configurational dependence of the magnetization dynamics in spin valve systems: Influence of spin pumping and domain wall induced coupling

R. Salikhov, R. Abrudan, F. Brüssing, K. Gross, C. Luo, K. Westerholt, and H. Zabel
Institut für Experimentalphysik/Festkörperphysik, Ruhr-Universität Bochum, 44780 Bochum, Germany

F. Radu
Helmholtz Zentrum Berlin für Materialien und Energien, Albert-Einstein-Str.15, 12489 Berlin, Germany

I. A. Garifullin
Zavoisky Physical-Technical Institute, Kazan Scientific Center of Russian Academy of Sciences, 420029 Kazan, Russia
(Received 30 July 2012; published 31 October 2012)

Using time-resolved x-ray resonant magnetic scattering we report on the precessional dynamics of spin valve systems with parallel (P) and antiparallel (AP) orientation of the ferromagnetic layers separated by a nonmagnetic spacer layers. Previously we observed in Co/Cu/$Ni_{81}Fe_{19}$(Py) spin valve systems an increase of the magnetic damping parameter in Py with changing magnetization direction of Py and Co layers from P to AP orientation [Salikhov *et al.*, Appl. Phys. Lett. **99**, 092509 (2011)]. We attributed this finding to the configurational dependence of the spin pumping effect [Kim and Chappert, J. Magn. Magn. Mater. **286**, 56 (2005)]. Here we extend our earlier findings by investigating the temperature dependence of the spin pumping effect and possible other causes for the configurational dependence of the damping parameter, such as domain wall induced coupling or magnetic dipole coupling. The main focus is on Co/Cu/Py trilayers and on Co_2MnGe/V/Py trilayers with spin valve properties.

DOI: 10.1103/PhysRevB.86.144422 PACS number(s): 75.78.−n, 72.25.Mk, 75.60.−d, 78.70.Ck

I. INTRODUCTION

Spin current related phenomena in F1/N/F2 trilayer structures, where F1 and F2 are ferromagnetic layers and N is a nonmagnetic metal layer, are an important topic of modern magnetism and can be used in many different practical applications like nonvolatile memory and spin wave electronics. For example, one can drive a spin-polarized electron current through the interface between the F1 and N layers and induce a magnetization torque in the F2 layer that can lead to magnetization reversal of F2.[1,2] The inverse effect, namely a spin current created by a precession of the magnetization in an externally applied magnetic field, also exists.[3] This so-called spin pumping effect may also lead to practical applications such as, e.g., a spin battery operated by ferromagnetic resonance (FMR).[4]

It has been shown that magnetization precession at F/N interfaces causes injection of spin polarization into nonmagnetic metals (N). If N is characterized by high spin relaxation rates, this injection may lead to additional damping of the magnetization precession in F.[5] It has also been found that in case of F1/N/F2 spin valve systems, the layer F1 may act as a sink for transverse spin current pumped by the F2 layer through the N spacer.[6] Thus, the F1 layer opens an additional relaxation channel for the magnetization dynamics in F2. Thus, the precessing magnetization of F1 and F2 layers are in mutual contact through the N spacer by exchanging nonequilibrium spin current. Moreover, it has clearly been shown that when the precession frequencies of F1 and F2 layers are equal, the induced damping by the spin pumping effect is strongly suppressed, since equalized spin currents flow from F1/N and N/F2 interfaces in opposite directions and the net flow across both interfaces cancels out.[7]

Kim and Chappert[8] investigated theoretically the dynamical coupling between the magnetic moments in F1/N/F2 structures by the spin pumping effect and concluded that this coupling may lead to a dependence of the magnetic relaxation on the mutual orientation of the magnetization direction of ferromagnetic layers. They reasoned that in the parallel (P) configuration the counter-propagating spin currents from the F1/N and N/F2 interfaces partially compensate each other, whereas in the antiparallel (AP) state they add, yielding an additional contribution to the precessional damping. This offers a unique possibility to control the relaxation rate of F2 by adjusting the relative magnetization direction of F1 and F2 from the P to the AP configuration.

Recently we have studied Co/Cu/$Ni_{81}Fe_{19}$ (Py) trilayers using time-resolved x-ray resonant magnetic scattering (tr-XRMS) at the synchrotron radiation facility BESSY II of the Helmholtz Zentrum Berlin.[9] A noticeable increase in the magnetic precessional damping parameter of the Fe magnetic moments in the Py layers was found when changing the mutual magnetization direction of the Py and Co layers from P to AP, whereas the magnetization precessional frequency did not change. We attributed this finding to the configurational dependence of the coupling induced by spin pumping between two ferromagnetic layers separated by a nonmagnetic metallic spacer, as predicted in Ref. 8. At the same time, Joyeux *et al.*[10] studied Py/Co/Cu/Co/MnIr spin valves using vector-analyzer based ferromagnetic resonance. They also found an increase of the resonance linewidth of the free ferromagnetic layer when the two ferromagnetic layers were in the AP state. In accordance with our conclusions they attributed the observed changes to the spin pumping effect.

In the present paper we show that in certain cases a domain-wall (DW) induced coupling mechanism can also be responsible for the configurational dependence of the damping of the free F layer in spin valve systems. The origin of this mechanism is magnetostatic coupling of the ferromagnetic

layers *via* DW-induced stray fields. The effect of stray fields from DWs in one F layer lowering the nucleation field in the other layer was noted previously by Fuller *et al.*[11] For the following discussions let us assume that F1 is the hard magnetic layer and F2 is the soft layer. Recently Thomas *et al.*[12] have observed that repeated motion of DWs in the soft ferromagnetic layer F2 of a F1/N/F2 trilayer can demagnetize the hard magnetic layer F1, even if the field used for the reversal is much smaller than the coercive field of F1. Vogel *et al.*[13,14] using x-ray photoelectron emission microscopy (X-PEEM) have shown that stray fields of DWs in F1 can decrease the nucleation barrier in the soft layer F2, resulting in a sizeable increase of the local switching speed of F2. Finally, Lew *et al.*[15] observed that interlayer DW coupling can induce a mirror domain structure in the magnetic trilayers. As one may note from this short overview, in a spin valve F1/N/F2 system, the inversion of the magnetization direction in F2 from P to AP direction may affect the nucleation and arrangement of DWs in F1 *via* DW stray fields. Then, having F1 in a domain state after inversion of the magnetization in F2, stray fields from the DWs in F1 can have a demagnetizing effect on the F2 layer and, simultaneously, can influence the magnetization dynamics in F2. For example the inhomogeneity of the demagnetizing fields from the DWs of F1 may lead to higher values of the magnetization precessional damping parameter in F2. Micromagnetic simulations[13,14] show that the influence of stray fields from DWs in spin valve systems can be considerable for spacer thicknesses (N) as large as 100 nm.

Here we present results of the configurational dependence of the damping of the Py magnetic moment in Co/Cu/Py trilayers, measured by tr-XRMS at low temperatures (100 K). We also show that in a spin valve structure consisting of Co_2MnGe/V/Py trilayer the DW induced coupling mechanism dominates the precessional relaxation rate when changing the configuration from P to AP. Experimentally, the origin of the configurational dependence of magnetic damping of the soft ferromagnetic layer in F1/N/F2 spin valves can be revealed by comparing the magnetization precessional frequency for the P and AP configurations.

II. EXPERIMENTAL DETAILS

Time resolved x-ray resonant magnetic scattering was originally proposed by Bailey *et al.*[16] This method allows measurements of the free precessional decay of the magnetization in ferromagnetic films in response to a field pulse excitation. The detection of the magnetic moment in the F films is based on the well-known x-ray magnetic circular dichroism (XMCD), which allows element-specific measurements. The circular dichroism signal is obtained in reflection geometry near the angle of grazing incidence. The time resolution is achieved through pump-probe techniques. Fast rise-time magnetic field pulses (pump) are synchronized with a variable delay time with respect to the x-ray photon bunches (probe) from the storage ring.

The experimental setup of our time-resolved XRMS with a possibility to perform experiments at low temperatures was implemented using the ALICE chamber[17] at the synchrotron radiation facility BESSY II of the Helmholtz Zentrum in Berlin.[18,19] For our pump-probe experiments we use a stripline geometry to generate a magnetic field pulse in the sample region. The 350 μm wide stripline structures were lithographically shaped after the sample deposition. Fast rise-time current pulses are delivered from the pulse generator through the stripline and converted into a pulsed Oersted field (H_p) perpendicular to the stripe (and current) direction. Time resolution in our setup is mostly determined by the finite photon bunch length of about 50 ps. Time delay scans were performed using a longitudinally biased magnetization by an external magnetic field (bias field H_b) from 7 to 35 Oe along the stripline. The free precessional frequency of the permalloy layer at a field of 35 Oe does not exceed 1.5 GHz, therefore the delay time between the current pulses and photon bunches was chosen to be $\tau = 100$ ps, which is higher than the resolution limit.

The stripline is oriented perpendicular to the scattering plane of the x-ray beam. Using circular polarized light in reflection geometry we are sensitive to the magnetization direction parallel to the scattering plane, thus we can monitor the evolution of the projection of the magnetization perpendicular to the stripline after pulse excitation by varying the delay time between current pulse and photon bunches. The use of a tandem undulator beamline at BESSY II allows adjusting the slits for the x-ray beam with a spot size of 100 μm at the sample position without loss in intensity for the detection of the XRMS. All samples were aligned with the x-ray beam focused in the middle of its longitudinal and lateral directions of the stripline.

The experiments were performed during single bunch operation mode of the synchrotron. In order to exclude effects from long term time drifts of the x-ray beam intensity (beam instability), we improved the detection technique by using a Lock-In amplifier. We modulate the switching pulse process ("pulse on"-"pulse off") of the pulse generator by a frequency of 1 Hz and the Lock-In technique accumulates the difference between the amplitudes of a photodiode current, which is proportional to the intensity reflected from the sample. For this purpose the pulse field was switched on and off (reference signal)[18] and integrated over five oscillations. After each change of the delay time a waiting time of 10 s was used to guarantee a stable signal. With this improvement we could significantly increase the signal to noise ratio of our scans and reduce the effect of long time fluctuations.

The Co/Cu/Py and Co_2MnGe/V/Py trilayers used for the present study were prepared on 10×10 mm sapphire (Al_2O_3) a-plane substrates. The Co/Cu/Py systems were deposited by magnetron sputter deposition in the MAGSSY preparation chamber with a base pressure of 3×10^{-8} mbar at room temperature. Applying a static magnetic field of 1000 Oe along the substrate *c* axis [0001] during the deposition process creates an effective uniaxial magnetic anisotropy for the Py and Co layers in the film plane. A 5 nm thick Pt seed layer was deposited prior to sputtering a 65 nm thick Cu conductive layer, which transforms the current pulse to a pulsed field H_p. On top of the thick Cu layer the Co/Cu/Py trilayers with a 25 or 40 nm thick Cu spacer layer was deposited. The thicknesses of the Co and Py layers were chosen to be 10 and 25 nm, respectively.

The Co_2MnGe/V/Py trilayers were prepared by RF sputtering at a substrate temperature of 300 °C. Instead of Cu we used V as a buffer (conducting) layer and spacer layer, to optimize the (110) textured growth of the ferromagnetic Heusler phase Co_2MnGe with structural order and flat interfaces. For details of thin films growth, crystal structure, and magnetic properties of the Co_2MnGe Heusler alloy we refer to Refs. 20 and 21. The nominal thicknesses of the films were Al_2O_3 (substrate)/V (40 nm)/Co_2MnGe (30 nm)/V (20 nm)/Py (15 nm)/V (4 nm). In a final step the samples were capped by 5 nm Al_2O_3 to prevent them from oxidation.

The 350 μm wide stripline structures were fabricated by electron-beam lithography and subsequent ion beam etching. For the lithographic processes we employed a FEI QUANTA 200 FEG scanning electron microscope in combination with a Elphy Quantum e-beam control using a negative resist. The striplines were oriented along the [0001] substrate axis, i.e., parallel to the direction of applied magnetic field during film deposition. Thus the magnetic easy axis of the Py layers is oriented parallel to the stripe axis. The head and tail ends of the stripes were etched down to the Cu (or V) bottom layer, thereby providing electrical contacts for the current pulses.

III. EXPERIMENTAL RESULTS

A. Co/Cu/Py spin valve

In Fig. 1(a) a magnetic hysteresis loop is presented for the Co/Cu (40 nm)/Py sample measured at a temperature of 100 K by SQUID magnetometery. The spin-valve-like character of the hysteresis loop with the extended plateaus of antiparallel orientation of the magnetization vectors in the adjacent F layers is clearly visible. The coercive field of the Co layer at 100 K is about $H_c = 48$ Oe, definitely larger than the room temperature value of $H_c \approx 18$ Oe.[9] This gives us the possibility to measure and compare the precession of the Py magnetic moment for the P and AP configurations to much higher values of the magnetic field (H_b) than is possible at room temperature. As seen from the hysteresis loops, the AP configuration can be achieved in two different ways: first by saturating the magnetization of both layers at positive fields and reversing the direction of the external field to negative values between the coercive fields of the Py and Co layers (descending branch of the hysteresis loop). Second, by saturating at negative fields and setting the field at positive values between the two coercive fields (ascending branch of the hysteresis loop). When comparing the results of tr-XRMS measurements of Co/Cu/Py samples performed in the AP state at positive and negative fields, we obtain identical behavior for the Py magnetization precession at the same absolute value of the external magnetic field. For the P-configuration scan at each particular bias field the tr-XRMS measurement was performed at positive fields after saturation at high positive fields.

In Figs. 1(b) and 1(c) we present the results on the magnetization precession of the Py layer in the Co/Cu (40 nm)/Py sample at $H_b = 11$ Oe (black open circles) and $H_b = 22$ Oe (blue closed circles) in the P and AP configuration, measured at 100 K. The photon energy was set to the Fe L_3 resonance edge (708 eV). Qualitatively one clearly sees that for both

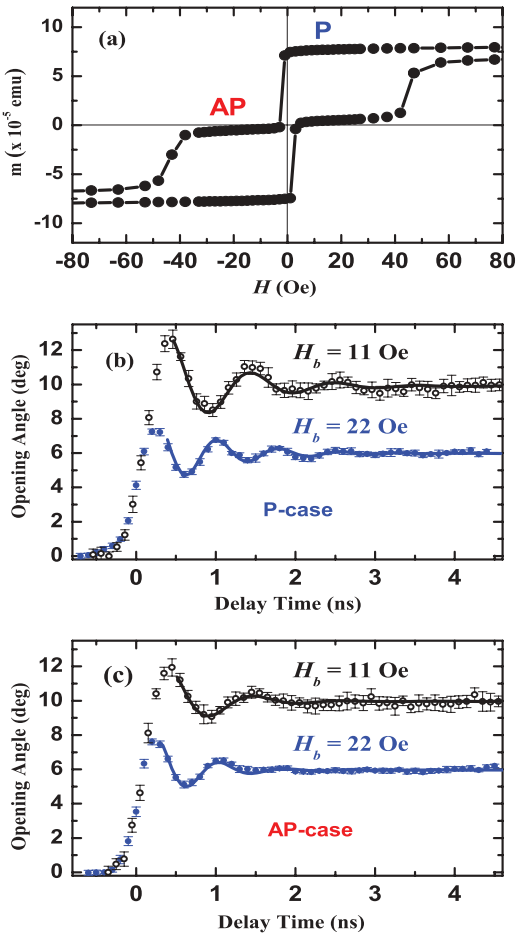

FIG. 1. (Color online) (a) Hysteresis loop for a Co/Cu(40 nm)/Py spin valve measured at 100 K. The bottom figures represent the precessional dynamics of the Py layer of the same sample measured at 100 K in the P configuration (b) and the AP configuration (c) for two different values of the bias field $H_b = 11$ Oe (black open circles) and 22 Oe (blue closed circles). The solid lines represent the fitting curves (see main text).

applied fields in the AP configuration the precession of the magnetization is damped faster than in P configuration, whereas the precessional frequency is identical in both cases. The damped oscillations in Figs. 1(b) and 1(c) result as the response to a steplike excitation of the pulsed Oersted field H_p, converted into time dependent opening angles of the Fe magnetic moments in Py, plotted as a function of delay time. The opening angles are defined by the vector sum of the bias field and the pulse field and can be varied by sweeping the bias field.[16,18,19] The solid lines in Figs. 1(b) and 1(c) represent a fit to the experimental data points using the solution of the Landau-Lifshitz (LL) equation adapted to our experimental conditions. For the fitting we follow the work of Crawford *et al.*[22] and Silva *et al.*,[23] where the magnetization dynamics of Py films as a response to a step pulse was measured magneto-optically and inductively.

After the quasistep excitation the solution of the LL equation is given by

$$\psi(t) = \psi_0 + \beta_0 \exp(-t\lambda/2)\sin(\omega_p t + \phi), \qquad (1)$$

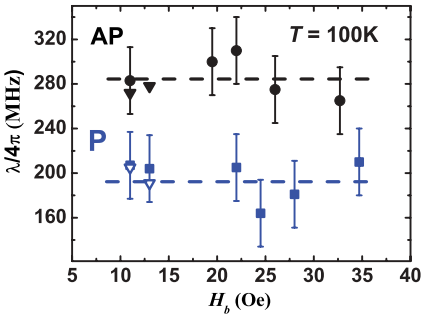

FIG. 2. (Color online) Landau-Lifshitz damping parameter $\lambda/4\pi$ obtained from the theoretical fit (see main text) as function of the bias field, where the delay scans have been performed. The delay scans of the Co/Cu (40 nm)/Py spin valve were measured at 100 K in the P configuration (blue squares) and AP configuration (black circles). The dashed lines represent a linear fit as guide to the eye. The triangles represent values of the damping parameters at room temperature, open blue triangles belong to the P configuration, closed black triangles to the AP configuration.

where ψ_0 is a steady-state equilibrium magnetization angle (opening angle), λ is the step damping constant, and $f_p = \omega_p/2\pi$ is the precessional frequency. The fitting parameters β_0 and ϕ were introduced to take into account the presence of a finite rise time of H_p.[23] In order to avoid spurious effects due to the deviation of the actual pulse shape from a perfect step function that would affect the fit parameters, we selected the data points at the delay times beyond the first maximum for the fitting.

Values of the LL damping parameter $\lambda/4\pi$ as a function of the bias field for the P (blue squares) and AP (black circles) configuration of Co and Py magnetization in Co/Cu (40 nm)/Py sample, as obtained from the fit, are presented in Fig. 2. The dashed lines represent an average value of the damping parameters. From Fig. 2 one can see that for H_b up to 35 Oe the damping in the AP state is higher than in the P state, with an estimated difference of 83 MHz. The damping parameters for the sample with the Cu spacer of 25 nm thickness (not shown) are virtually identical. Values of the damping parameters obtained from the room temperature (300 K) measurements[9] are also presented in Fig. 2 as open blue triangles (P configuration) and closed black triangles (AP configuration). Within the error bars of our experiment, we did not notice any changes in the damping parameter of Py either in the P or the AP configuration for temperatures ranging from 300 K to 100 K.

B. Co_2MnGe/V/Py spin valve

The magnetic hysteresis loop measured at room temperature for Co_2MnGe (30 nm)/V (20 nm)/Py (15 nm) sample is shown in Fig. 3(a). One can recognize from its shape that the Heusler alloy layer reverses its magnetization gradually, in contrast to the Co layers in Co/Cu/Py [Fig. 3(b)] which exhibits a narrow range of external field (2–3 Oe) for the magnetization reversal. Therefore one may conclude that in the Co_2MnGe layer the magnetization reversal proceeds *via* multiple intermediate domain states.

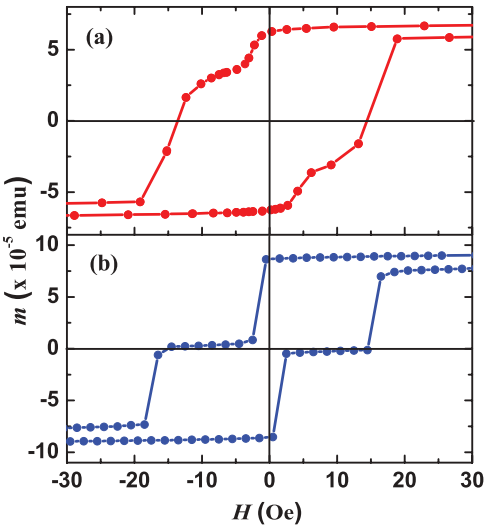

FIG. 3. (Color online) Hysteresis loop of (a) Co_2MnGe (30 nm)/V (20 nm)/Py (15 nm) spin valve and (b) Co (10 nm)/Cu (25 nm)/Py (25 nm) spin valve, measured by SQUID magnetometery at room temperature.

Results of the tr-XRMS measurements of the magnetization dynamics of the Py layer in Co_2MnGe/V/Py at $H_b = 13$ Oe for the P configuration (closed blue circles) and for the AP configuration (open black circles) with respect to the initial magnetization direction in Co_2MnGe layer are presented in Fig. 4(a). From the fit of these curves we obtain the change in LL damping parameter $\lambda/4\pi$ from 208 MHz for the P state to about 224 MHz for the AP configuration. Furthermore, we notice a change of the precessional frequency f_p from 1.01 GHz for the P configuration to 0.88 GHz for the AP configuration. This is in strong contrast to the case of Co/Cu/Py where the precessional frequency $f_p = 0.9$ GHz is identical for the P and the AP configuration [Fig. 4(b)].

The obtained values of precessional frequency and damping of Py magnetic moment in Co_2MnGe/V/Py trilayer at different values of H_b for the P (blue circles) and AP configurations (black squares) are plotted in Figs. 5(a) and 5(b). For all values of the bias field one can see that in the AP case, where the Co_2MnGe layer is supposed to be in a magnetic domain state,

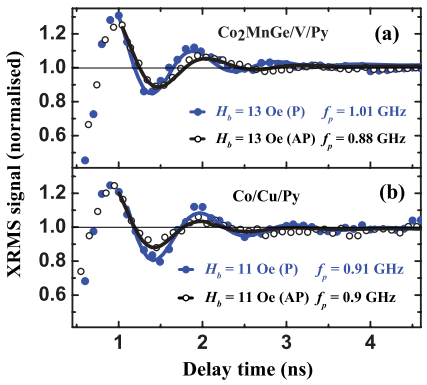

FIG. 4. (Color online) Comparison of magnetization precessional dynamics in the Py layer at room temperature: (a) for Co_2MnGe/V/Py trilayer measured at the bias field $H_b = 13$ Oe, (b) for Co/Cu/Py spin valve measured at $H_b = 11$ Oe.

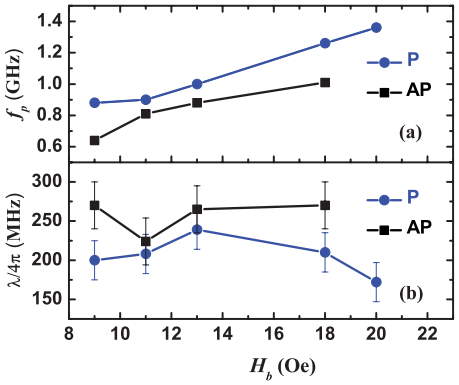

FIG. 5. (Color online) (a) Precessional frequency f_p and (b) damping parameter $\lambda/4\pi$ in the P configuration (blue circles) and AP configuration (black squares) for the Co_2MnGe (30 nm)/V (20 nm)/Py (15 nm) spin valve as function of the bias field H_b. Solid lines are guides to the eye.

the precessional frequency is always smaller and the damping parameter is lager as compared to the P state. Moreover, from Fig. 5 we infer that a larger difference in f_p correlates with a larger difference in $\lambda/4\pi$.

IV. DISCUSSION

As evident in Figs. 1(b) and 1(c), the precession of the magnetic moment in the Py layer, measured at 100 K, is damped faster when oriented antiparallel to the magnetic moment of the Co layer than when being in the parallel orientation, similar to what has been observed in these samples at room temperatures.[9] This difference is present for all AP configurations [see hysteresis loop in Fig. 1(a)] up to a bias field of 35 Oe (Fig. 2). In Ref. 9 we discussed the possible mechanisms responsible for this change in the damping parameter for the P and AP configurations, and concluded that the dominating mechanism is the spin pumping effect. The domain wall (DW) induced coupling mechanism was not explicitly considered. However, our tr-XRMS measurements on the Co_2MnGe/V/Py system indicate that in some cases DW coupling may also be of importance for explaining the damping mechanism.

From the shape of the hysteresis loop in Fig. 3(a) one may conclude that in the AP configuration for a bias field of 13 Oe, where the tr-XRMS measurements have been performed, the Co_2MnGe layer is in a magnetic multidomain state. Thus stray fields emanating from the DWs of the Co_2MnGe layer additionally contribute to the bias field H_b and to a corresponding change in the Py magnetization precessional frequency f_p, according to the Kittel equation.[24] This contribution is clearly visible in our experiment. Simultaneously, the intrinsic inhomogeneity of dipolar stray fields causes an increase of the damping parameter. This fact is well known in ferromagnetic resonance (FMR) experiments as inhomogeneous broadening of the resonance linewidth.[25] The higher the strength of the inhomogeneous stray field, the higher is the difference one would expect for P and AP state in both the precessional frequency f_p and the damping parameter $\lambda/4\pi$, a correlation which is clearly visible in Fig. 5.

Interestingly, the precessional frequency f_p in the AP state is systematically smaller than the one for the P configuration where the Co_2MnGe layer is in a single domain state (Fig. 5). This shows that in the AP configuration the magnetic domains in the Co_2MnGe layer are arranged in a manner that their stray fields are mostly aligned opposite to the direction of magnetization of the Py layer and thus reduce the external magnetic field in the Py layer and the value of the precessional frequency. In other words, the DWs in the Heusler layer produce an effective dipolar magnetic field in the Py layer with a direction opposite to the direction of the magnetic moment in Py. This stray field has the tendency to break up the single domain state of the Py layer into a multidomain state, a situation which is known in F1/N/F2 trilayers as the mirror domain state.[15] As an additional evidence for this type of magnetic coupling we mention that the coercive fields of the Co_2MnGe and Py layers in the spin valve samples are definitely larger than in single Co_2MnGe and Py layers, indicating that both ferromagnetic layers contribute to the magnetization reversal of each other.

In contrast, for the Co/Cu/Py trilayers we do not see a difference in the magnetization precession frequency of the Py magnetic moment for the P and AP configuration [Fig. 4(b)], indicating that the stray field from domain walls of the Co layer does not noticeably influence the dynamics of the Py magnetization and, consequently, does also not appreciably contribute to the difference in the damping parameter between P and AP configuration. Therefore the dominating mechanism responsible for the observed change of the LL damping parameter of the Py layer is the spin pumping effect.

The configurational dependence of the magnetic damping in spin valves can be understood in terms of the model proposed by Joyeux *et al.*[10] In the P configuration the magnetizations of both ferromagnetic layers precess with the same rotational sense, so that two counter-propagating spin polarized currents pumped into the N layer carry spin vectors with a mutual orientation constant in time. At each time instant, the total spin vector seen by the soft ferromagnetic layer is the difference of the counter-propagating spin vectors, such that there is partial cancellation. The situation is different for the AP configuration. In this state the dynamic magnetization of the two layers rotates in opposite rotational sense, such that the two counter-propagating spin currents carry spin vectors that rotate in opposite sense; in this situation the total spin vector varies in time and never cancels. This leads to a strong dynamic coupling between the two layers and an additional damping of the precessional motion.

We discuss next the temperature and thickness dependence of the damping parameter. It has been shown in Ref. 10 that in Py/Co/Cu/Co/MnIr spin valves with a Cu spacer layer thickness of 4 nm the change in damping of the free ferromagnetic layer for the P and AP configurations is almost independent of temperature. In our Co/Cu/Py trilayers the thickness of Cu spacers is 25 nm and 40 nm, therefore the spin-diffusion regime for the spin current should be considered.[6] The spin-diffusion length λ_s is a measure of the spin momentum decay across the Cu spacer. If the spacer layer is significantly thinner than λ_s, the spin-current propagation can be considered to be in the spin ballistic regime. It is known that the spin-diffusion length in Cu is very large with values

at room temperature reaching 350 nm,[26–28] which is almost 10 times larger than the Cu thickness in our samples. According to our measurements of the electrical resistivity, the mean free path of conduction electrons in the Cu spacers for our samples changes little when lowering the temperature from 300 K to 100 K. Therefore the corresponding values of λ_s should be almost identical. This is confirmed by our measurements of tr-XRMS at low temperatures, showing that the LL damping parameter of the Py layer does not change between 300 K and 100 K either in the P or AP configuration (Fig. 2). The fact that we do not obtain any difference in the damping parameter for samples with different Cu spacer thicknesses also indicates that the spin diffusion length in these layers is indeed large compared to the selected thicknesses of 25 and 40 nm.

V. CONCLUSION

In conclusion, we have studied the free precessional magnetization dynamics in spin valves of the type F1/N/F2 with different coercive field values for changing the magnetization direction in F2 (Py) versus F1 (Co,Co_2MnGe) from parallel to antiparallel. Using time resolved x-ray resonant magnetic scattering we have determined the precessional frequency and the precessional damping in the P and AP configuration. In case of Co/Cu/Py spin valves we find that the damping parameter in the AP configuration is considerable larger than in the P state. This effect is independent of the Cu spacer layer thickness and independent of the temperature in the considered range of 25–40 nm and 100–300 K, respectively. Furthermore, we noticed that in Co/Cu/Py spin valves the precessional frequency f_p is independent of the mutual orientation of the layer magnetization. We take the configurational dependence of the damping parameter together with the configurational independent precessional frequency as clear evidence for the spin pumping effect, which is an additional damping contribution to the usual spin-lattice relaxation governed by two-way spin currents.

For Co_2MnGe/V/Py spin valve systems we again find the characteristic difference in the damping parameters for the P and AP configurations. However, in contrast to Co/Cu/Py, we determined a lower precessional frequency in the AP state as compared to the P state. From this difference in the precessional frequency we infer that an additional magnetic field acts on the magnetic layers, which likely is due to domain wall coupling in the domain state of the sample. Therefore we conclude that if the precessional frequency is identical for the P and AP configuration, as observed for our Co/Cu/Py system [Fig. 4(b)], mainly the spin pumping effect is responsible for the configurational change of the damping parameter. In contrast, a sizable configuration dependence of the precessional frequency, as observed in the Co_2MnGe/V/Py system, points towards a domain wall coupling, which may also affect the difference in the damping parameter between the P and AP states.

ACKNOWLEDGMENTS

This work is supported by BMBF 05K10PC1. We are also thankful to the Helmholtz Zentrum Berlin for travel support under BMBF 05 ES3XBA/5.

[1] J. C. Slonczewski, J. Magn. Magn. Mater. **159**, L1 (1996).
[2] L. Berger, Phys. Rev. B **54**, 9353 (1996).
[3] Y. Tserkovnyak, A. Brataas, G. E. W. Bauer, and B. I. Halperin, Rev. Mod. Phys. **77**, 1375 (2005).
[4] A. Brataas, Y. Tserkovnyak, G. E. W. Bauer, and B. I. Halperin, Phys. Rev. B **66**, 060404(R) (2002).
[5] Y. Tserkovnyak, A. Brataas, and G. E. W. Bauer, Phys. Rev. Lett. **88**, 117601 (2002).
[6] O. Mosendz, G. Woltersdorf, B. Kardasz, B. Heinrich, and C. H. Back, Phys. Rev. B **79**, 224412 (2009).
[7] B. Heinrich, Y. Tserkovnyak, G. Woltersdorf, A. Brataas, R. Urban, and G. E. W. Bauer, Phys. Rev. Lett. **90**, 187601 (2003).
[8] J.-V. Kim and C. Chappert, J. Magn. Magn. Mater. **286**, 56 (2005).
[9] R. Salikhov, R. Abrudan, F. Brüssing, St. Buschhorn, M. Ewerlin, D. Mishra, F. Radu, I. A. Garifullin, and H. Zabel, Appl. Phys. Lett. **99**, 092509 (2011).
[10] X. Joyeux, T. Devolder, Joo-Von Kim, Y. Gomez de la Torre, S. Eimer, and C. Chappert, J. Appl. Phys. **110**, 063915 (2011).
[11] H. W. Fuller and D. L. Sullivan, J. Appl. Phys. **33**, 1063 (1962).
[12] L. Thomas, M. G. Samant, and S. S. P. Parkin, Phys. Rev. Lett. **84**, 1816 (2000).
[13] J. Vogel, W. Kuch, R. Hertel, J. Camarero, K. Fukumoto, F. Romanens, S. Pizzini, M. Bonfim, F. Petroff, A. Fontaine, and J. Kirschner, Phys. Rev. B **72**, 220402(R) (2005).
[14] J. Vogel, W. Kuch, K. Fukumoto, F. Romanens, S. Pizzini, and J. Camarero, Appl. Phys. A **92**, 505 (2008).
[15] W. S. Lew, S. P. Li, L. Lopez-Diaz, D. C. Hatton, and J. A. C. Bland, Phys. Rev. Lett. **90**, 217201 (2003).
[16] W. E. Bailey, L. Cheng, D. J. Keavney, C.-C. Kao, E. Vescovo, and D. A. Arena, Phys. Rev. B **70**, 172403 (2004).
[17] J. Grabis, A. Nefedov, and H. Zabel, Rev. Sci. Instrum. **74**, 4048 (2003).
[18] St. Buschhorn, F. Brüssing, R. Abrudan, and H. Zabel, J. Synchrotron Radiat. **18**, 212 (2011).
[19] St. Buschhorn, F. Brüssing, R. Abrudan, and H. Zabel, J. Phys. D **44**, 165001 (2011).
[20] A. Bergmann, J. Grabis, B. P. Toperverg, V. Leiner, M. Wolff, H. Zabel, and K. Westerholt, Phys. Rev. B **72**, 214403 (2005).
[21] K. Gross, P. Szary, O. Petracic, F. Brüssing, K. Westerholt, and H. Zabel, Phys. Rev. B **84**, 054456 (2011).
[22] T. M. Crawford, T. J. Silva, C. W. Teplin, and C. T. Rogers, Appl. Phys. Lett. **74**, 3386 (1999).
[23] T. J. Silva, C. S. Lee, T. M. Crawford, and C. T. Rogers, J. Appl. Phys. **85**, 7849 (1999).
[24] C. Kittel, *Introduction to Solid State Physics* (Wiley, New York, 1986).
[25] B. Heinrich, *Spin Relaxation in Magnetic Metallic Layers and Multilayers*, Vol. III (Springer, New York, 2004).
[26] F. F. Jedema, A. T. Filip, and B. J. van Wees, Nature (London) **410**, 345 (2001).
[27] F. F. Jedema, H. B. Heershce, A. T. Filip, J. J. A. Baselmans, and B. J. van Wees, Nature (London) **416**, 713 (2002).
[28] S. Yakata, Y. Ando, T. Miyazaki, and S. Mizukami, Jpn. J. Appl. Phys. **45**, 3892 (2006).